VNU Journal of Science: Mathematics - Physics
Journal homepage: https://js.vnu.edu.vn/MaP

Original Article

Numerical Analysis of Optical Properties Using Octagonal Shaped $Ge_{15}As_{15}Se_{17}Te_{53}$ Chalcogenide Photonic Crystal Fiber

Nguyen Thi Thuy*

University of Education, Hue University, 34 Le Loi, Hue City, Vietnam

Received 7 September 2023
Revised 25 December 2023; Accepted 22 April 2024

Abstract: A novel $Ge_{15}As_{15}Se_{17}Te_{53}$ chalcogenide-based photonic crystal fiber with octagonal cladding was designed which exhibits low confinement loss and high nonlinearity. The dispersion properties were investigated over a wide wavelength range of up to 11 µm. Based on preliminary simulation results, three fibers with suitable characteristic quantities are proposed for supercontinuum generation. Among these fibers, fiber #F_1 (Λ = 3.1 µm, d/Λ = 0.3) exhibits all-normal dispersion with a small value of −0.374 ps/[nm.km]. At the same time, the highest nonlinear coefficient of 2876.861 $W^{-1}.km^{-1}$ at the pump wavelength of 5.45 µm is also found. The #F_2 fiber (Λ= 4.5 µm, d/Λ = 0.3) has anomalous flat dispersion with one zero dispersion wavelength. This fiber has the smallest dispersion and lowest confinement loss values of 0.281 ps/[nm.km] and 1.360×10^{-9} at 5.7 µm pump wavelength, respectively. With the anomalous dispersion, #F_3 fiber (Λ = 3.5 µm, d/Λ = 0.3) offers a small effective mode area of 20.892 μm^2 and a low confinement loss of 4.974×10^{-8} dB/m at 5.25 µm wavelength. The proposed fibers can possess a low peak power, broadband supercontinuum source, suitable for application fields such as optical communication and biomedical sensors.

Keywords: $Ge_{15}As_{15}Se_{17}Te_{53}$ photonic crystal fibers, octagonal cladding, flat dispersion, high nonlinear coefficient, low confinement loss.

1. Introduction

The versatility of the photonic crystal fiber (PCF) in terms of morphology, application, and the glass used for fabrication enables its geometries to be optimized with both dispersion and nonlinear properties [1]. As the best nonlinear medium for supercontinuum generation (SCG), PCFs have a wide range of applications in science and technology, including the fields of optical communication,

* Corresponding author.
E-mail address: ntthuy@hueuni.edu.vn

https//doi.org/10.25073/2588-1124/vnumap.4873

telecommunication, spectroscopy, medical, security, petrochemical industries, biomedical sensing, etc [2, 3]. During last several decades, there are many attempts to improve the dispersion and nonlinear properties of silica-PCF, including altering the cladding shape [4-6], modifying the structural parameters [7, 8], or using highly nonlinear fluids to fill their hollow cores [5-7]. Even so, the SCG spectrum expansion based on the PCFs is still limited, making it difficult for application areas in infrared ranges. This obstacle is due to pure silica having a high phonon energy of about 1,100 cm^{-1} [9].

Recently, chalcogenide glasses (ChG) have become one of the favored highly nonlinear substrate materials for PCFs, attracting widespread interest in the design of infrared SCG sources. The major inorganic components of ChG include Sulfur (S), Selenium (Se), Tellurium (Te) along with the addition of other elements from group XV such as Arsenic (As) and Antimony (Sb); and group XIV such as Germanium (Ge) and Silicon (Si) [10]. The unique combination of ChG's attractive optical properties (the high linear refractive index, high nonlinear refractive index, low phonon energy, and great optical transparency extending from the visible region to 20 μm [10] with the design flexibility of PCFs) makes ChG-PCF be an excellent nonlinear medium for SCG sources. A large amount of evidence from both theoretical and experimental shows great potential applications of ChG PCF in infrared (MIR) regions, such as in the fields of biomedicine and pollution monitoring [8-10], because most molecules exhibit distinctive spectral fingerprints in this region for their differential vibrational absorption originating from chemical bonds or functional groups.

With a star arrangement of air holes in the hexagonal lattice, authors of [8] introduced two $Ge_{11.5}As_{24}Se_{64.5}$-PCFs with flat dispersion, the dispersion interval of 71.42 and 36.31 ps/[nm.km]. Furthermore, the confinement loss is less than 2.30×10^{-7} dB/km for PCF_1 and 3.50×10^{-2} dB/km for PCF_2 in the wavelength range of 1,000–6,000 nm. With the triangular lattice, authors of [11] verified that $Ga_8Sb_{32}S_{60}$-based ChG-PCFs has flat and all-normal dispersion properties. Moreover, for the fiber ($\Lambda = 2.5$ μm, $d_1/\Lambda = 0.352$), the effective mode area and the nonlinear coefficient at the center wavelength of 4.5 μm were found to be of 15.23 μm^2 and 970 $W^{-1}.km^{-1}$, respectively. By varying the diameters of the air holes in the cladding, the authors [12] also obtained an all-normal dispersion with a value of −35 ps/[nm.km] at the wavelength 3 μm for $Ge_{15}Sb_{15}Se_{70}$-PCF with $d = 0.8$ μm. Besides, the proposed fiber for SCG exhibited high nonlinear coefficients up to 1.96 $W^{-1}.km^{-1}$ at the same wavelength. The increased filling factor d/Λ leads to an increase in the dispersion curve as demonstrated in [13] with the $As_{39}Se_{61}$-PCFs. Besides, an all-normal dispersion regime with a peak close to the zero dispersion can be achieved for $d = 0.7$. This fiber also gives a small effective mode area of 6.8 μm^2 and a high nonlinear coefficient of 5.89 $W^{-1}.km^{-1}$ at a wavelength of 3.45 μm. An ultra-flattened near-zero dispersion was presented in [14] with liquid-filled As_2S_3-PCF. In [15] authors proposed a rectangular core $Ga_8Sb_{32}S_{60}$-PCF with a flat dispersion profile, high nonlinearity, and low effective mode area. The recommended fiber for SCG has geometrical parameters $d_1 = 1.6$ μm, $d_2 = 0.5$ μm, and $\Lambda = 2.5$ μm with a dispersion value of −15.54 ps/[nm.km] at pump wavelength 4 μm. Its nonlinear coefficient and effective mode area at the same pump wavelength are 853 $W^{-1}.km^{-1}$ and 22.8 μm^2, respectively. The multicomponent $GeSe_2$-As_2Se_3-PbSe based PCF in [16] offered the dispersion with zero dispersion wavelength (ZDW) around 4.2 μm. The value of dispersion at 3.1 μm is of 100 ps/[nm.km] for optimized parameters $d = 1.3$ μm and $\Lambda = 2.5$ μm. However, the nonlinear coefficients of these PCFs are not high, about only few hundred $W^{-1}.km^{-1}$. As can be seen, the ChG substrate materials used to design PCF are very diverse. Each PCF exhibits optical characteristics consistent with broadband SCG. However, some PCFs also have large dispersion values, the nonlinear coefficients are not as high as expected, which significantly affects the quality of SCG. Even some complex lattice structures may make PCFs fabrication difficult in future.

In this work, we designed solid-core PCFs based on $Ge_{15}As_{15}Se_{17}Te_{53}$ with octagonal lattice of eight rings of air holes arranged in the regular arrangement in the cladding. The variation in air hole diameter

changed the dispersion of the PCFs in the wide wavelength region up to 11 μm, which is valuable for broad-spectrum SCGs in MIR regions. All-normal and anomalous dispersions with multiple ZDWs were found. We have also obtained small effective mode areas and higher nonlinear coefficients of 2,000 $W^{-1}.km^{-1}$ with the proposed PCF for SCG. In particular, these PCFs provide very low confinement loss values, averaging around 10^{-8} dB/m. These attractive optical properties can contribute to improved performance of SCG processes including further spectral expansion in infrared regions, high flatness, and low noise.

2. Numerical Modeling of the PCFs

Many works focus on the variety of geometric structures of cladding (star, triangular, hexagonal, circular, square, rectangular lattices, etc.) [8, 11, 15] or the variation in the size of air holes (hole diameters and distance between them), this helps the optical properties to be investigated in detail, thereby proposing many optimal structures. These structures have been shown to enhance SCG process performance. In [7], the dispersion and nonlinear properties of circular and octagonal ChG-PCF were compared to propose the optimal structure for the SCG process. From this idea, we proposed $Ge_{15}As_{15}Se_{17}Te_{53}$-based octagonal lattice PCFs to investigate their optical properties based on numerical simulations, thereby proposing optimal PCFs for SCG.

In this section, the solid-core PCFs consisting of an eight-ring octagonal lattice with circular air holes are considered. We have optimized the structural parameters for all rings of air holes in the cladding to achieve the desired dispersion. The lattice constant Λ has a value of 3.1 μm, 3.5 μm, 4.5 μm, and 5.0 μm. The diameter d of the air holes varies according to the formula $d = (0.3-0.75)\Lambda$, in 0.5 steps. The solid core with diameter D_c is calculated as $D_c = 2\Lambda - d$. The size of the core should be controlled to ensure that it is not too small to make it difficult to fabricate the fiber, nor too large to guide the light in the core well. Figure 1 presents a cross-section of the PCF, in which the air holes are arranged at regular intervals and parallel to the axis of the core.

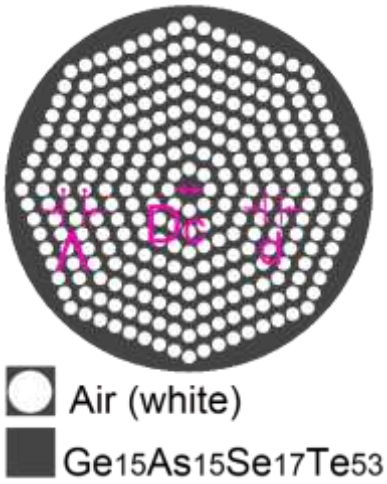

Figure 1. The cross-sections of $Ge_{15}As_{15}Se_{17}Te_{53}$-PCF with an octagonal lattice.

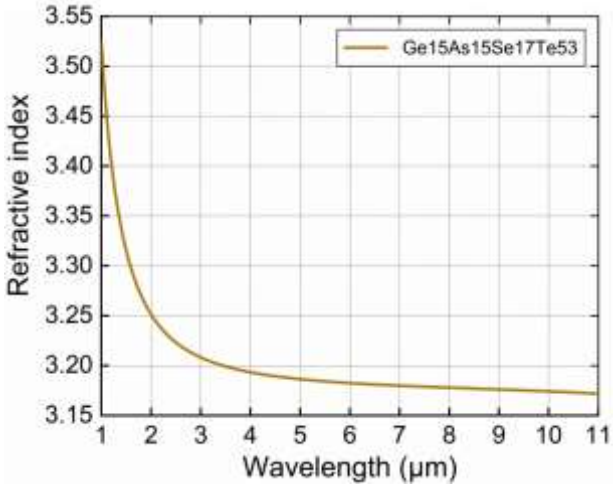

Figure 2. The values of the refractive index of $Ge_{15}As_{15}Se_{17}Te_{53}$ is extrapolated using Sellmeier's equation.

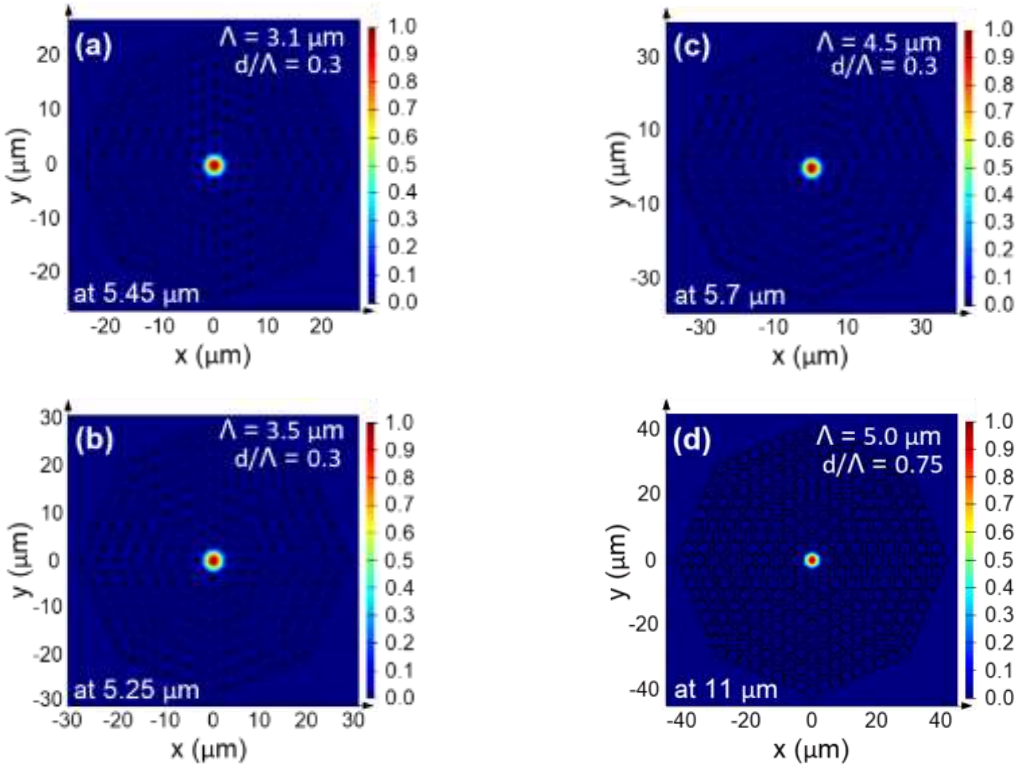

Figure 3. Light is well confined in the core of $Ge_{15}As_{15}Se_{17}Te_{53}$-PCFs with several different structures.

We use Lumerical Mode Solution software with the full-vector finite-difference eigenmode (FDE) method [17] to simulate the structure of PCFs. $Ge_{15}As_{15}Se_{17}Te_{53}$ glass is chosen as the substrate material because it has a wide transparent wavelength range extending from 0.8 to 20 μm, and has a linear refractive index two orders of magnitude higher than that of silica [18]. In addition, it has a high solubility and a low phonon energy when doped with rare-earth elements [19]. To collect wavelength-dependent refractive index data of $Ge_{15}As_{15}Se_{17}Te_{53}$ for the system, we use the Sellmeier coefficient from Eq. 1 [18]. The refractive index of $Ge_{15}As_{15}Se_{17}Te_{53}$ is extrapolated using Sellmeier's equation, which is verified in Figure 2. The refractive index decreases with increasing survey wavelength, but in the shorter wavelength region from 1 to 3.5 μm, the refractive index decreases more.

$$n = \sqrt{1 + \frac{9.0823\lambda^2}{\lambda^2 - 0.2049} + \frac{-0.000003\lambda^2}{\lambda^2 - 27.093} + \frac{0.03\lambda^2}{\lambda^2 - 218.28}} \quad (1)$$

The optical properties of PCFs in the wavelength range of 1.0 – 11.0 μm are investigated by solving Maxwell's wave equations with the boundary condition that is the perfectly matched layers. The FDE method helps to divide the cross-section of the microfiber into hundreds of thousands of rectangles to absorb light waves from the calculated region without any reflection. Figure 3 shows the well-contained light image in the core of the PCFs.

The fast or slow propagation of the frequency components of the input pulse is characterized by dispersion *D*, given by the following formula [20]:

$$D(\lambda) = -\frac{\lambda}{c}\frac{d^2 \mathrm{Re}[n_{\mathrm{eff}}]}{d\lambda^2} \tag{2}$$

where Re[n_{eff}] is the real part of the effective index of the guided mode, λ and c are the wavelengths and the speed of light in a vacuum, respectively.

As light propagates in an optical fiber, the power will gradually decrease with the propagation distance, which is characterized by the confinement loss. The smaller the confinement loss, the more beneficial it is for the SCG process. The confinement loss (L_c) is calculated through the wavelength (λ) and the imaginary part of the effective refractive index (Im[n_{eff}]) according to the following formula [20].

$$L_c = 8.686\frac{2\pi}{\lambda}\mathrm{Im}[n_{\mathrm{eff}}] \tag{3}$$

The degree of light confined in the core of the PCFs can be calculated through the amplitude of the transverse electric field E propagating inside the fiber, which is characterized by the effective mode area (A_{eff}). This is also an important parameter that affects the broadening of the SC spectrum at the edge of the pulse. In addition, the nonlinearity of the optical fiber is also computed through the effective mode area. The smaller the effective mode region of the PCF, i.e. the larger the nonlinear coefficient (γ), the broader the SCG spectrum and the lower the peak power of the input pulse. The effective mode area and the nonlinear coefficient are determined according to the following formulas [20]:

$$A_{\mathrm{eff}} = \frac{\left(\int_{-\infty}^{\infty}\int_{-\infty}^{\infty}|E|^2\,dxdy\right)^2}{\int_{-\infty}^{\infty}\int_{-\infty}^{\infty}|E|^4\,dxdy} \tag{4}$$

$$\gamma(\lambda) = 2\pi\frac{n_2}{\lambda A_{\mathrm{eff}}} \tag{5}$$

where $n_2 = 44.5\times10^{-18}$ m^2/W, is the nonlinear refractive index of $Ge_{15}As_{15}Se_{17}Te_{53}$ material.

3. Simulation Results and Analysis

Dispersion is one of the important properties of PCFs, in SCG it governs the possibility of occurrence of nonlinear effects when injecting fibers with all-normal or anomalous dispersion profiles. From there, it decides the characteristics of the SCG. Figure 4 presents the dispersion properties of the $Ge_{15}As_{15}Se_{17}Te_{53}$-PCFs according to the variation of structural parameters including Λ and d/Λ. Dispersion properties are quite variable with all-normal and anomalous dispersion with many ZDWs. For PCFs with small cores (Λ = 3.1 µm), the dispersion is only available in the wavelength region from 1.0 to 8.0 µm, with only one all-normal dispersion observed with d/Λ = 0.3. The dispersion curves that gradually shift above the zero-dispersion line, become anomalous dispersion with one or two ZDWs when d/Λ increases. For Λ = 3.5 µm, all the dispersion curves are anomalous. We found two anomalous dispersion curves with two ZDWs (d/Λ = 0.3 and 0.35) in the investigated wavelength region up to 9 µm. When investigating dispersion properties with Λ = 4.5 and 5.0 µm, the wavelength region wide up to 11 µm, all structures have anomalous dispersion profiles with one ZDW. In general, ZDW_{1s} tend to shift toward shorter wavelengths while the ZDW_{2s} move toward longer wavelengths as d/Λ increases (Table 1). For SCG, this makes it easier to choose the wavelength to pump the fiber in mid-infrared and infrared regions.

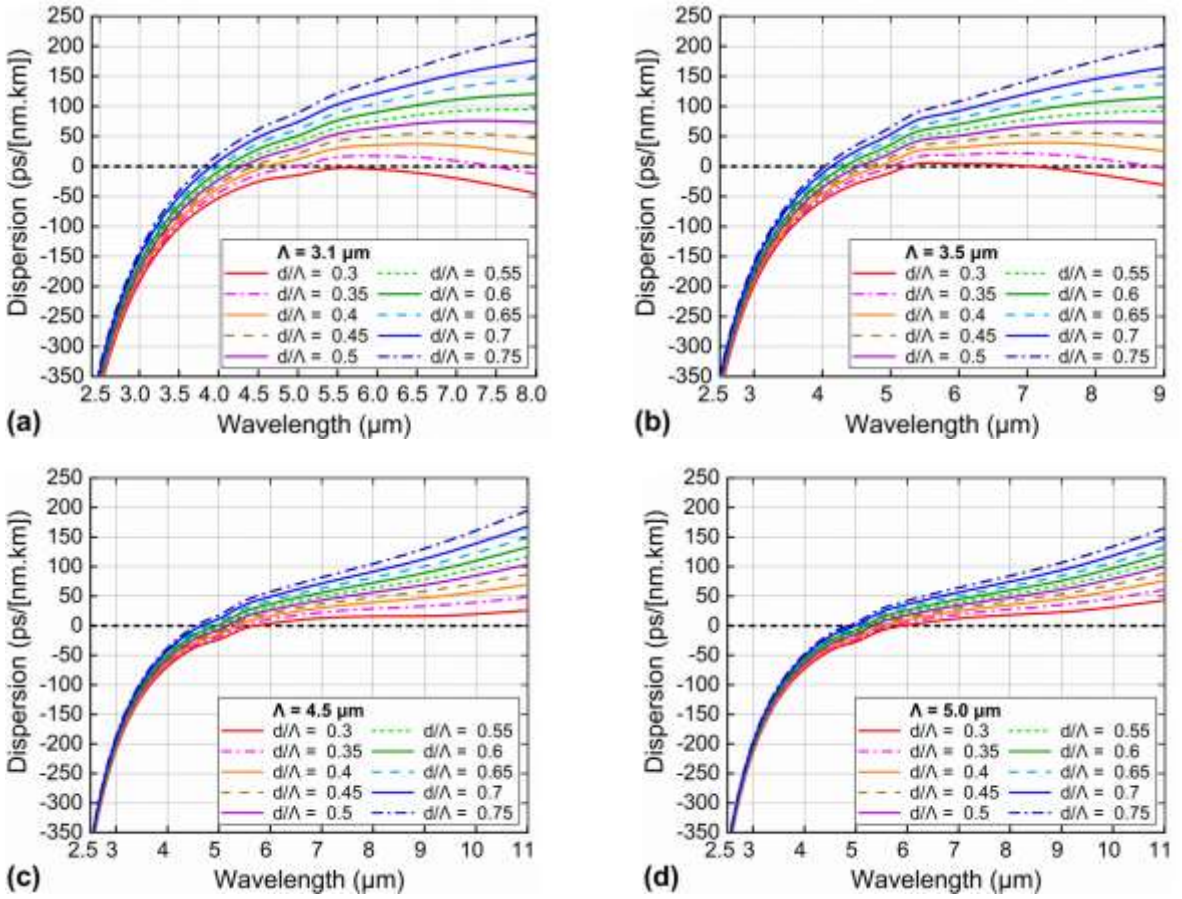

Figure 4. The dispersion properties of the Ge15As15Se17Te53-PCFs with various values of d/Λ and Λ = 3.1, 3.5, 4.5 and 5.0 μm.

Table 1. The ZDW of the $Ge_{15}As_{15}Se_{17}Te_{53}$-PCFs with various values of d/Λ and Λ = 3.1, 3.5, 4.5 and 5.0 μm

d/Λ	Λ = 3.1 μm		Λ =3.5 μm		Λ = 4.5 μm	Λ = 5.0 μm
	ZDW_{1s}	ZDW_{2s}	ZDW_{1s}	ZDW_{2s}	ZDW_{1s}	ZDW_{1s}
0.3	D < 0	D < 0	5.212	7.128	5.678	5.913
0.35	5.050	7.483	5.032	8.832	5.406	5.603
0.4	4.583		4.847		5.322	5.432
0.45	4.420		4.654		5.248	5.373
0.5	4.296		4.529		5.174	5.311
0.55	4.194		4.425		5.104	5.251
0.6	4.088		4.315		5.014	5.186
0.65	3.998		4.225		4.798	5.117
0.7	3.905		4.132		4.636	5.046
0.75	3.811		4.030		4.536	4.844

When the dispersion curve has a flat section, it is easier to enforce phase matching between different wave packets over a long period causing new frequencies to be generated via cross-phase modulation (XPM) or four-wave mixing (FWM) [21]. The spectrum will be divided into two sections with normal and anomalous dispersion if ZDW exists. When pumping the fiber in the normal dispersion regime, the self-phase modulation (SPM) effect dominates the spectral expandability and often produces a highly coherent spectrum. In order to increase the coherence of the spectrum, it is common to choose optical fibers possessing an all-normal dispersion profile. Meanwhile, the soliton dynamics are suppressed because the energy is sequentially transferred from high to low frequencies in the pulse by stimulated Raman scattering (SRS). If the fiber is pumped in the anomalous dispersion regime, the spectral expansion is mainly due to the soliton dynamics through effects such as SPM, soliton fission (SF), soliton self-frequency shift (SSFS), and dispersive waves (DWs) [22]. More, because the phase modulation (XPM) and four-wave mixing (FWM) are generated to the left of the ZDW, a green shift in the trapped wave is produced. For fibers with anomalous dispersion with two ZDWs, the dispersion region is divided into three sections by two ZDWs (this means a part of abnormal dispersion in between two parts with normal dispersion). Then, SSFS with a clear redshift boundary is closer to the second ZDW than PCF with one ZDW [23]. The redshift in the DW is due to the presence of a negative dispersion gradient near the second ZDW in the normal dispersion region and in the trapped wave [24]. This is caused by the phase matching between the redshift soliton and the redshift DW. "The former effect extends the SCG spectrum to the red end, while the latter flattens the supercontinuum between the redshift soliton and the redshift DW" [25]. Furthermore, the presence of XPM and FWM can be on each side of each ZDW which can further increase the bandwidth [26]. Therefore, it is very important to control the width and slope of each dispersion region depending on the adjustment for the number and position of ZDWs in the dispersion curve.

The preliminary data on the dispersion characteristics of $Ge_{15}As_{15}Se_{17}Te_{53}$-PCFs suggest that we recommend three fibers with suitable dispersion that can generate low peak power, broadband supercontinuum. The dispersion properties of the three proposed fibers, are verified in Figure 5a. The first fiber, #F_1 (Λ= 3.1 μm, d_1/Λ = 0.3) has an all-normal dispersion in the wavelength range 1.0−8.0 μm. It is a typical parabolic dispersion profile with the local maximum around wavelength 5.45 μm. We also choose the pump wavelength at this value to optimize the dispersion value. With a low dispersion value of −0.374 ps/[nm.km] at a wavelength of 5.45 μm, this fiber is expected to generate the broadband, highly coherent SCG under the dominance of the SPM effect followed by optical wave breaking (OWB). Possessing the flat anomalous dispersion with one ZDW (ZDW_1 = 5.678 μm), the second fiber (Λ = 4.5 μm, d/Λ = 0.3) has the smallest dispersion value of 0.281 ps/[nm.km] at 5.7 μm wavelength in three proposed fibers. The soliton dynamics including SRS, SF, SSFS, and DW will be the main mechanisms that govern the width and the flatness of the spectrum. The spectrum will be very broad but the noise will be more than SCG using #F_1 fiber. The interaction of XPM, FWM, and DW nonlinear effects will result in a broadband SCG spectrum as the third fiber #F_3 (Λ = 3.5 μm, d/Λ = 0.3) has anomalous dispersion with the two separate ZDWs far apart (ZDW_1 = 5.212 μm, ZDW_2 = 7.128 μm). The proposed pump wavelength is 5.25 μm, very close to ZDW_1. At this wavelength, fiber #F_3 shows a small dispersion value of 2.156 ps/[nm.km]. We have achieved a smaller dispersion value than some publications [8, 12, 15, 16] using ChG as a substrate material to study the optical properties of PCFs for SCG.

The confinement loss of the proposed fibers varies very little in the wavelength region from 1 to 6 μm for #F_1 fiber, from 1 to 7 μm for #F_3 fiber, and from 1 to 11 μm for #F_2 fiber, which is depicted in Figure 5b. In long wavelength regions, the L_c value increases very quickly (the large gradient) because the low frequency components make it difficult to enter the core of the PCFs, resulting in poor light confinement in the core. However, the maximum value of L_c is about 10^{-2} dB/m, which is still much lower than that of some silica-based solid-core PCFs. This is also the great advantage of these

$Ge_{15}As_{15}Se_{17}Te_{53}$-based PCFs compared to other substrates. $\#F_2$ fiber has the lowest loss among the three fibers, a L_c value of 1.360×10^{-9} dB/m at a pump wavelength of 5.7 µm. The L_c values of $\#F_1$ and $\#F_3$ fibers are 2.523×10^{-6} and 4.974×10^{-8} at 5.45 µm and 5.25 µm the pump wavelengths, respectively. The increase of L_c in the long wavelength region is likely to limit the development of the SCG spectrum toward the red edge. However, this limitation is not expected to be large because the L_c values of all three fibers are very low in this wavelength region.

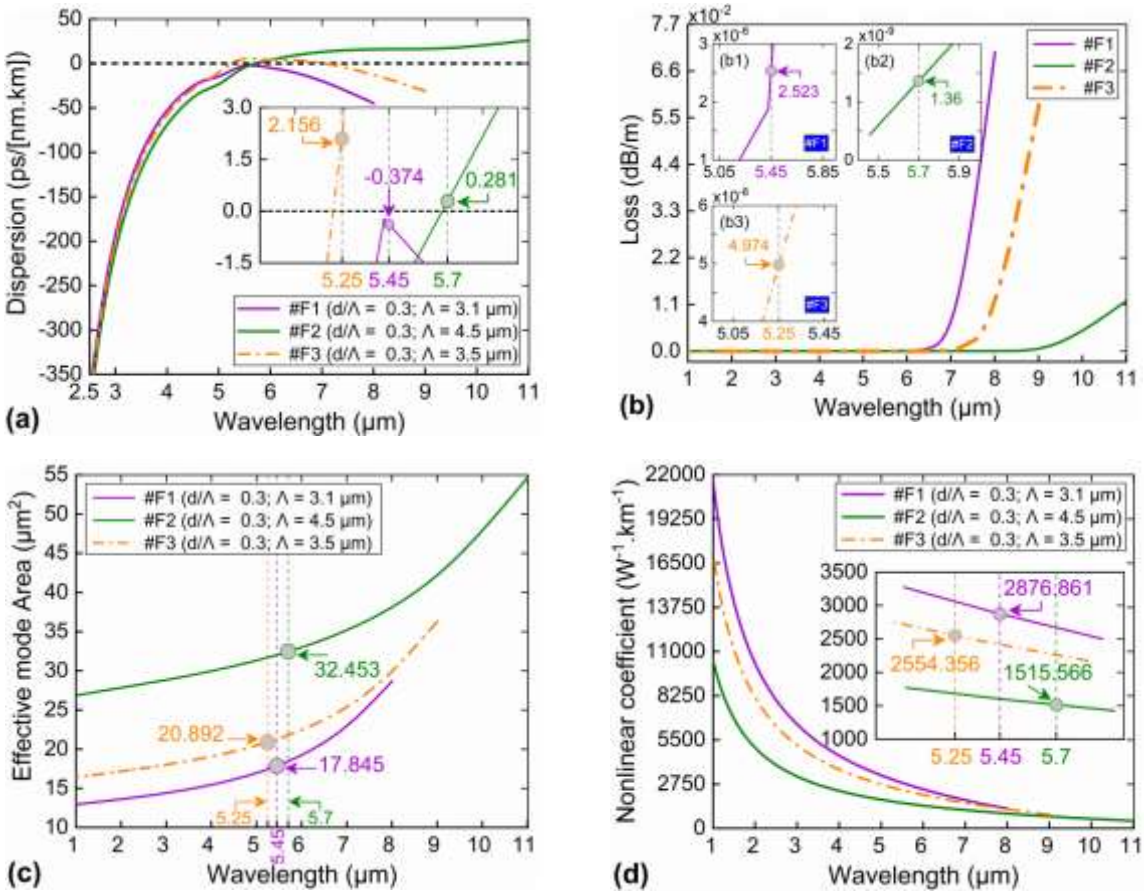

Figure 5. The optical properties of the proposed fibers $\#F_1$, $\#F_2$, and $\#F_3$.

The relationship between the effective mode area and the nonlinear coefficient vs. wavelength is plotted as shown in Figure 5c and 5d. The effective mode area increases with increasing wavelength. In the long wavelength region, low frequency components easily leak from the core to the cladding or between air holes, which reduces the nonlinear coefficient and increases the effective mode area (because the nonlinearity is inversely proportional to the effective mode area). Fiber $\#F_2$ has the largest A_{eff} value in the entire survey wavelength range, that is, has the lowest nonlinear coefficient. We obtained the small A_{eff} and high γ values at suitable pumping wavelengths for fibers $\#F_1$, $\#F_2$, and $\#F_3$. The values are verified in Table 2. With a value of 2876.861 $W^{-1}.km^{-1}$, 1515.566 $W^{-1}.km^{-1}$, 2554.356 $W^{-1}.km^{-1}$, these fibers will be the low peak power SCG sources. It should also be noted that it is difficult to simultaneously optimize the optical properties of PCFs. Depending on different application purposes, it is possible to optimize several different optical properties of PCFs accordingly.

Table 2. The structural parameters and the values at the pump wavelengths of the characteristic quantities of three proposed fibers

#	D_c (μm)	Λ (μm)	d/Λ	Pump wavelength (μm)	A_{eff} (μm^2)	γ (W^{-1}.km^{-1})	D ps/[nm.km]	L_c (dB/m)
#F_1	5.27	3.1	0.3	5.45	17.845	2876.861	−0.374	2.523×10^{-6}
#F_2	7.65	4.5	0.3	5.7	32.453	1515.566	0.281	1.360×10^{-9}
#F_3	5.95	3.5	0.3	5.25	20.892	2554.356	2.156	4.974×10^{-8}

During the process of investigating the optical properties of $Ge_{15}As_{15}Se_{17}Te_{53}$-PCFs, we find it difficult to simultaneously optimize the characteristic quantities. For example, fiber #F_2 has flat anomalous dispersion, the smallest dispersion value and the lowest confinement loss at the pump wavelength. This helps the SCG spectrum using #F_2 to be as wide as possible, which is a favorable condition for applications in the MIR range [27]. However, the nonlinear coefficient of this fiber is not high. The SCG spectrum can still be maximally expanded but requires a large input pulse peak power. Fiber #F_1 has the highest nonlinearity coefficient but also exhibits the highest confinement loss. The SCG process may require only low peak power but the spectral broadening towards the red side may be limited. The SCG process with ChG-PCF with all-normal dispersion usually gives a broad spectrum, flat top, and high coherence. This makes these PCFs an excellent candidate for various important MIR region applications including MIR spectroscopy, medical imaging, optical coherence tomography and materials characterization [11]. Similarly, although the dispersion value is the largest, fiber #F_3 has a higher nonlinearity coefficient than fiber #F_2. This fiber will be the low peak power SCG sources to help save costs. Its SCG spectrum will be broadened due to soliton dynamics. However, this fiber has two ZDWs, so the dispersion region will be divided into three parts. The SCG spectrum can be further expanded thanks to the displacement of solitons between the dispersion regions [23-26]. Therefore, it depends on each specific application field to optimize the appropriate optical properties. Table 3 also compares the values of characteristic quantities at the pump wavelength with other works on ChG-based PCF.

Table 3. The comparison of the values of characteristic quantities at the pump wavelength with other works on ChG-based PCF

#	Pump wavelength (μm)	A_{eff} (μm^2)	γ (W^{-1}.km^{-1})	D ps/[nm.km]	L_c (dB/m)	Ref.
#F_1	5.45	17.845	2876.861	−0.374	2.523×10^{-6}	This work
#F_2	5.7	32.453	1515.566	0.281	1.360×10^{-9}	This work
#F_3	5.25	20.892	2554.356	2.156	4.974×10^{-8}	This work
$Ga_8Sb_{32}S_{60}$-PCF	4.5	15.23	970	–	–	[11]
$Ge_{15}Sb_{15}Se_{70}$-PCF	3.0	–	1960	−35	–	[12]
$As_{39}Se_{61}$-PCF	3.45	6.8	5890	–	–	[13]
$Ga_8Sb_{32}S_{60}$-PCF	4.0	22.8	853	15.54	–	[15]
$Ge_{11.5}As_{24}S_{64.5}$-PCF	4.0	13.1	340	5.17	50	[28]

4. Conclusion

The skillful adjustment of the structural parameters in the design of solid-core $Ge_{15}As_{15}Se_{17}Te_{53}$-PCFs with octagonal lattice has helped to optimize the dispersion and optical properties, which are

necessary for SCG applications. Obtained results of this work again veryfy that the dispersion and nonlinear properties of fibers can also be well controlled through the lattice parameters where the cladding geometry plays an important role [21-23]. We have studied in detail the dispersion properties of 40 structures, the diversity of dispersion properties gives the fiber a higher chance of being selected for SCG. Each fiber introduced has suitable dispersion properties to enhance SCG generation efficiency. All three proposed fibers have small dispersion values, nonlinear coefficients as high as thousands of W−1.km−1, even about three times larger than that reported in [11, 15], about 8 times larger compared to the one in [27]. Furthermore, very low confinement loss, as low as 1.360×10^{-9} dB/m at the pump wavelength of 5.7 μm is the outstanding advantage of these fibers. These are favorable conditions for broadband and low peak power SCG. The pump wavelengths chosen above 5.0 μm in consideration of the local maximum of the dispersion curve, are all in the MIR range, which is quite useful for applications in this region. The proposed fibers are suitable for broadband SCG with diverse nonlinear effects depending on the all-normal or anomalous dispersion properties. They can be useful sources of SCG in optical communication and biomedical sensing applications.

References

[1] L. Thévenaz, Advanced Fiber Optics: Concepts and Technology, EPFL Press, New York, EBook ISBN: 9780429156335, 2011, https://doi.org/10.1201/b16404.

[2] M. Pi, C. Zheng, R. Bi, H. Zhao, L. Liang, Y. Zhang, Y. Wang, F. K. Tittel, Design of a Mid-Infrared Suspended Chalcogenide/Silica-on-Silicon Slot-Waveguide Spectroscopic Gas Sensor with Enhanced Light-Gas Interaction Effect, Sensor and Actuators B: Chemical, Vol. 297, 2019, pp. 126732, https://doi.org/10.1016/j.snb.2019.126732.

[3] D. Wasserman, R. Singh, T. Akalin, Special Issue on Mid-Infrared and THz photonics, Journal of Optics, Vol. 16, 2014, pp. 090201, https://doi.org/10.1088/2040-8978/16/9/090201.

[4] T. N. Thi, D. H. Trong, L. C. Van, Supercontinuum Generation in Ultra-Flattened Near-Zero Dispersion PCF with C_7H_8 Infiltration, Optical and Quantum Electronics, Vol. 55, 2023, pp. 93, https://doi.org/10.1007/s11082-022-04351-x.

[5] T. N. Thi, L. C. Van, Supercontinuum Spectra Above 2700 nm in Circular Lattice Photonic Crystal Fiber Infiltrated Chloroform with The Low Peak Power, Journal of Computational Electronics, 2023, pp. 31, https://doi.org/10.1007/s10825-023-02078-w.

[6] T. N. Thi, L. C. Van, Supercontinuum Generation Based on Suspended Core Fiber Infltrated with Butanol, Journal of Optics, 2023, pp. 15, https://doi.org/10.1007/s12596-023-01323-6.

[7] K. C. Selva, R. Anbazhagan, Investigation on Chalcogenide and Silica Based Photonic Crystal Fibers with Circular And Octagonal Core, AEU - International Journal of Electronics and Communications, Vol. 72, 2017, pp. 40-45, https://doi.org/10.1016/j.aeue.2016.11.018.

[8] M. Z. Alam, M. I. Tahmid, S. T. Mouna, M. A. Islam, M. S. Alam, Design of a Novel Star Type Photonic Crystal Fiber for Mid-Infrared Supercontinuum Generation, Optics Communications, Vol. 500, No. 1, 2021, pp. 127322, https://doi.org/10.1016/j.optcom.2021.127322.

[9] X. Zou, T. Izumitani, Spectroscopic Properties and Mechanisms of Excited State Absorption and Energy Transfer Upconversion for Er^{3+}-Doped Glasses, Journal Non-Crystalline Solids, Vol. 162, No. (1-2), 1993, pp. 68-80, https://doi.org/10.1016/0022-3093(93)90742-G.

[10] D. Jayasuriya, C. R. Petersen, D. Furniss, C. Markos, Z. Tang, M. S. Habib, O. Bang, T. M. Benson, A. B. Seddon, Mid-IR Supercontinuum Generation in Birefringent, Low Loss, Ultra-High Numerical Aperture Ge-As-Se-Te Chalcogenide Step-Index Fiber, Optical Materials Express, Vol. 9, No. 6, 2019, pp. 2617-2629, https://doi.org/10.1364/ome.9.002617.

[11] A. Medjouri, D. Abed, Z. Becer, Numerical Investigation of a Broadband Coherent Supercontinuum Generation in $Ga_8sb_{32}s_{60}$ Chalcogenide Photonic Crystal Fiber with All-Normal Dispersion, Opto-Electronics Review, Vol. 27, No. 1, 2019, pp. 1-9, https://doi.org/10.1016/j.opelre.2019.01.003.

[12] A. Medjouri, D. Abed, Mid-Infrared Broadband Ultraflat-Top Supercontinuum Generation in Dispersion Engineered Ge-Sb-Se Chalcogenide Photonic Crystal Fiber, Optical Materials, Vol. 97, 2019, pp. 109391, https://doi.org/10.1016/j.optmat.2019.109391.

[13] A. Medjouria, D. Abed, Design and Modelling of All-Normal Dispersion $As_{39}Se_{61}$ Chalcogenide Photonic Crystal Fiber for Flat-Top Coherent Mid-Infrared Supercontinuum Generation, Optical Fiber Technology, Vol. 50, 2019, pp. 154-164, https://doi.org/10.1016/j.yofte.2019.03.021.
[14] M. Kalantari, A. Karimkhani, H. Saghaei, Ultra-Wide Mid-IR Supercontinuum Generation in As_2S_3 Photonic Crystal Fiber by Rods Filling Technique, Optik, Vol. 158, 2018, pp. 142-151, https://doi.org/10.1016/j.ijleo.2017.12.014.
[15] P. Chauhan, A. Kumar, Y. Kalra, Mid-Infrared Broadband Supercontinuum Generation in a Highly Nonlinear Rectangular Core Chalcogenide Photonic Crystal Fiber, Optical Fiber Technology, Vol. 46, 2018, pp. 174-178, https://doi.org/10.1016/j.yofte.2018.10.004.
[16] P. Chauhan, A. Kumar, Y. Kalra, Numerical Exploration of Coherent Supercontinuum Generation in Multicomponent $GeSe_2$-As_2Se_3-PbSe Chalcogenide Based Photonic Crystal Fiber, Optical Fiber Technology, Vol. 54, 2020, pp. 102100, https://doi.org/10.1016/j.yofte.2019.102100.
[17] S. Guo, F. Wu, S. Albin, H. Tai, R. S. Rogowski, Loss and Dispersion Analysis of Microstructured Fibers by Finite-Difference Method, Optics Express, Vol. 12, No. 15, 2004, pp. 3341-3352, http://dx.doi.org/10.1364/OPEX.12.003341.
[18] N. Mi, B. Wu, L. Jiang, L. Sun, Z. Zhao, X. Wang, P. Zhang, Z. Pan, Z. Liu, S. Dai, Q. Nie, Structure Design and Numerical Evaluation of Highly Nonlinear Suspended-Core Chalcogenide Fbers, Journal of Non-Crystalline Solids, Vol. 464, 2017, pp. 44-50, http://dx.doi.org/10.1016/j.jnoncrysol.2017.03.025.
[19] A. Yang, M. Zhang, L. Li, Y. Wang, B. Zhang, Z. Yang, D. Tang, Ga–Sb–S Chalcogenide Glasses for Mid-Infrared Applications, J. Am. Ceram. Soc., Vol. 99, No. 1, 2016, pp. 12-15, http://dx.doi.org/10.1111/jace.14025.
[20] G. P. Agrawal, Nonlinear Fiber Optics (5^{th} Edition), Academic Press, Elsevier, 2013, ISBN: 978-0-12-397023-7, https://doi.org/10.1016/C2011-0-00045-5.
[21] D. S. Rao, R. Engelsholm, I. Gonzalo, B. Zhou, P. Bowen, P. Moselund, O. Bang, M. Bache, Ultra-Low-Noise Supercontinuum Generation with a Flat Near-Zero Normal Dispersion Fiber, Optics Letters, Vol. 44, No. 9, 2019, pp. 2216-2219, https://doi.org/10.1364/OL.44.002216.
[22] A. Rampur, D. M. Spangenberg, G. Stępniewski, D. Dobrakowski, K. Tarnowski, K. Stefańska, Temporal Fine Structure of All-Normal Dispersion Fiber Supercontinuum Pulses Caused by Non-Ideal Pump Pulse Shapes, Optics Express, Vol. 28, No. 11, 2020, pp. 16579-16593, https://doi.org/10.1364/OE.392871.
[23] D. V. Skryabin, F. Luan, J. C. Knight, P. S. J. Russell, Soliton Self-Frequency Shift Cancellation in Photonic Crystal Fibers, Science, Vol. 301, No. 5640, 2003, pp. 1705-1708, https://doi.org/10.1126/science.1088516.
[24] G. Genty, M. Lehtonen, H. Ludvigsen, Effect of Cross-Phase Modulation on Supercontinuum Generated in Microstructured Fibers with Sub-30 fs Pulses, Optics Express, Vol. 12, No. 19, 2004, pp. 4614-4624, https://doi.org/10.1364/OPEX.12.004614.
[25] Y. Huang, H. Yang, S. Zhao, Y. Mao, S. Chen, Design of Photonic Crystal Fibers with Flat Dispersion and Three Zero Dispersion Wavelengths for Coherent Supercontinuum Generation in both Normal and Anomalous Regions, Results in Physics, Vol. 23, 2021, pp. 104033, https://doi.org/10.1016/j.rinp.2021.104033.
[26] E. N. Tsoy, C. M. D. Sterke, Theoretical Analysis of The Self-Frequency Shift Near Zero-Dispersion Points: Soliton Spectral Tunneling, Physical Review A, Vol. 76, No. 4, 2007, pp. 043804, https://doi.org/10.1103/PhysRevA.76.043804.
[27] Y. Wu, M. Meneghetti, J. Troles, J. L. Adam, Chalcogenide Microstructured Optical Fibers for Mid-Infrared Supercontinuum Generation: Interest, Fabrication, and Applications, Appl. Sci., Vol. 9, No. 8, 2018, pp. 1637, https://doi.org/10.3390/app8091637.
[28] M. R. Karim, H. Ahmad, B. M. A. Rahman, Design and Modeling of Dispersion-Engineered All-Chalcogenide Triangular-Core Fiber for Mid Infrared-Region Supercontinuum Generation, Journal of Optical Society of Americal B, Vol. 35, No. 2, 2018, pp. 266-275, http://dx.doi.org/10.1364/JOSAB.35.000266.